

## Superconductivity and Characterization of the High-Pressure Reaction Products of Carbon Diselenide, CSe<sub>2</sub>

Akiko KOBAYASHI,\* Yukiyoishi SASAKI, Tokuko WATANABE,<sup>†</sup> Seiichiro IKEHATA,<sup>††</sup> Haruo KISHIDA,<sup>†††</sup> Haruki KAWAMURA,<sup>††††</sup> Reizo KATO,<sup>††††</sup> and Hayao KOBAYASHI<sup>††††,\*</sup>

Department of Chemistry, Faculty of Science, The University of Tokyo, Hongo, Bunkyo-ku, Tokyo 113

<sup>†</sup>The University of the Air, Wakaba, Chiba 260

<sup>††</sup>Department of Physics, Faculty of Science, The University of Tokyo, Hongo, Bunkyo-ku, Tokyo 113

<sup>†††</sup>Nissei Sangyo Co., Ltd., Toranomon, Minato-ku, Tokyo 105

<sup>††††</sup>National Research Institute for Metals, Sakura, Niihari, Ibaraki 305

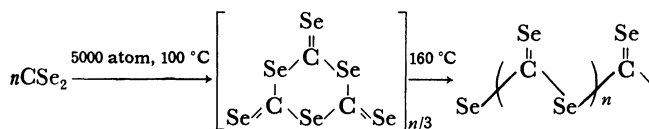
<sup>†††††</sup>Department of Chemistry, Faculty of Science, Toho University, Funabashi, Chiba 274

(Received May 13, 1986)

The physical properties and the structure of black solids obtained by the high-pressure reaction of CSe<sub>2</sub> were examined by IR, X-ray diffraction, scanning electron microscope, electron diffraction, thermal analyses and magnetic experiments. The crystalline solid, which was metallic ( $\sigma(RT) \approx 50 \text{ S cm}^{-1}$ ) at ambient pressure became superconductor above 20 GPa ( $T_c(\text{onset}) = 6 \text{ K}$ ), while the amorphous solid was insulating. Contrary to the previously proposed one- or two-dimensional polymerization structure of (CSe<sub>2</sub>)<sub>x</sub>, it has been revealed that the metallic CSe<sub>2</sub> sample have a rather complex structure that is composed of the crystalline hexagonal Se, graphite and some amorphous parts. Thus, the high conductivity and the diamagnetism of the crystalline solid at ambient pressure seems to come from graphite part and the superconductivity seems to come from hexagonal Se part. The superconducting transition behavior depended on the path of the pressure-cooling steps. The superconducting state was observed only when the pressure was increased at the low temperature.

Recent discoveries of many organic superconductors based on the multi-sulfur (or selenium)  $\pi$ -donor or  $\pi$ -acceptor molecules have aroused a considerable interest in the field of synthetic metals. Contrary to the traditional organic conductors with the disadvantage of the Peierls instabilities originated from their one-dimensionalities, in these multi-sulfur compounds the two-dimensional (or three-dimensional) intermolecular close contacts of chalcogen atoms in the  $\pi$ -conjugated molecules play a central role for the formation of the conduction bands. Carbon diselenide is the simplest  $\pi$ -conjugated molecule with Se atoms.

Okamoto and Wojciechowski reported that CSe<sub>2</sub> was polymerized into conductive amorphous solid ( $10^{-3} \text{ S cm}^{-1}$ ).<sup>1)</sup> Okamoto et al. proposed the two step reactions:



The second step appears to be analogous to the solid state polymerization of S<sub>2</sub>N<sub>2</sub>, into the well known inorganic polymer superconductor, (SN)<sub>x</sub>.<sup>2)</sup> Since the similar linear chain structure had been already suggested in the polymerization of CS<sub>2</sub> under a pressure of 30 kbar,<sup>3)</sup> this polymerization mechanism of CSe<sub>2</sub> seemed to be reasonable. We tried to obtain the similar polymer. Various types of the black solids were obtained.<sup>4,5)</sup> Most of them were amorphous but in some cases, highly conducting crystalline solids were obtained. This crystalline solid was revealed to exhibit a superconducting transition at high pressure.

Initially we proposed the two-dimensional polymerization model as to the crystalline solid,<sup>6)</sup> because the EXAFS analysis showed that the linear chain structure

model was incorrect. However, recently we have found the evidence of the existence of hexagonal Se and graphite in the conducting solid.

In this report, the electrical properties of the high pressure reaction products of CSe<sub>2</sub> and their characterization by X-ray diffraction, scanning electron microscope, chemical analysis, EXAFS, DSC, IR, electron microscope, electron diffraction, magnetic susceptibility and ESR experiments are described.

### Experimental

Carbon diselenide, CSe<sub>2</sub> is a toxic, malodorous and golden-yellow liquid reagent used in the synthetic studies of the  $\pi$ -donor molecules with the Se atoms, which was obtained by the reaction of Se vapor with dichloromethane in the nitrogen stream and the subsequent distillation.<sup>7)</sup> Liquid CSe<sub>2</sub> in the teflon cell was pressurized at about 5 kbar and heated to 80–100 °C for 2–3 h. Then the pressure was released and the cell was heated at 100–130 °C. Various types of black solids were obtained. About 0.3 ml of CSe<sub>2</sub> was used at a time. The degree of the crystallinity of the solid was very sensitive to the conditions of the preparation (pressure and temperature) and the reaction was hardly to control. When the reaction temperature was too high (130–160 °C), the amorphous solid was obtained. On the contrary, when the reaction temperature was below 70 °C, nonreacted CSe<sub>2</sub> was remained.

The conductivity measurements were performed by the fourprobe method with silver paint within the temperature range of 1.5 K to 300 K. The high-pressure resistivity experiments were performed on the compaction sample by the two probe method using the diamond anvil high-pressure cell.

The X-ray powder patterns were measured on a Rigaku X-ray powder diffractometer. Intensities were extremely weak and those data were obtained by scanning up to  $2\theta = 130^\circ$  (Cu K $\alpha$  radiation, Ni filter, 35 kV, 15 mA) for a week running (0.72°/h).

Temperature dependence of X-band ESR spectra from 100

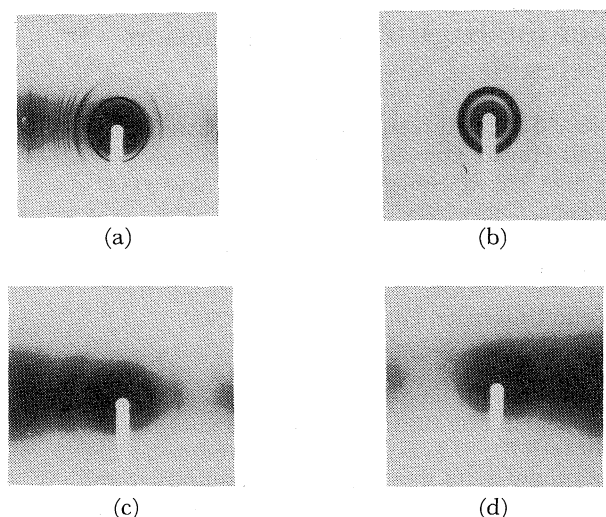


Fig. 1. X-Ray diffraction diagrams of high-pressure reaction products of  $\text{CSe}_2$ .

a): Metallic solid ( $50 \text{ S cm}^{-1}$ ), b): semiconducting ( $5 \text{ S cm}^{-1}$ ) solid, c): low-conducting solid ( $10^{-3} \text{ S cm}^{-1}$ ), d): insulating solid ( $10^{-8} \text{ S cm}^{-1}$ ).

to 300 K was examined on a JEX-FELIX ESR spectrometer with flowing liquid nitrogen gas. Skin effect of ESR was observed as to the metallic sample and the experiment was performed on the finely-ground powder sample.

Magnetic susceptibility of metallic sample was measured by a Faraday method on a powder sample of about 0.13 g over a temperature range between 2 and 296 K. A permanent magnet and electro-balance were used. The temperature of the sample was controlled through the pure helium gas at a pressure of about 3 Torr (1 Torr = 133.322 Pa). The helium gas was purified by passing through a charcoal trap held at 75 K.

The measurement of the EXAFS spectra was performed at the Photon Factory of National Laboratory for High Energy Physics (KEK-PF), using EXAFS facilities at the beam line 10-B with a Si(311) channel-cut monochromator.

The IR spectra were taken of a dispersion in KBr within the range of  $400 \text{ cm}^{-1}$  to  $4000 \text{ cm}^{-1}$ .

The thermogravimetric analyses were performed on a Rigaku differential scanning calorimeter within the temperature range between 20 to  $400^\circ\text{C}$ .

Electron microscope and electron diffraction experiments were performed on H-800 Hitachi Electron Microscope.

Scanning electron microscope experiments were made by using X-650 Hitachi Scanning Electron Microanalyser.

## Results and Discussion

**Electrical and Magnetic Properties.** As described before, black solids were prepared from  $\text{CSe}_2$ . By changing the applied pressure and the heating temperature, we obtained various solids. The X-ray diffraction diagrams of the products are shown in Fig. 1. There are various solids with different crystallinities. The conductivity of the compaction sample of the crystalline solid, which gave sharp X-ray diffraction patterns (Fig. 1a), was about  $50 \text{ S cm}^{-1}$  and the resistivity ratio at 1.7 K ( $\rho_{1.7}/\rho_{300}$ ) was 2–3 (Fig. 2a). This small resistivity ratio and almost linear temperature

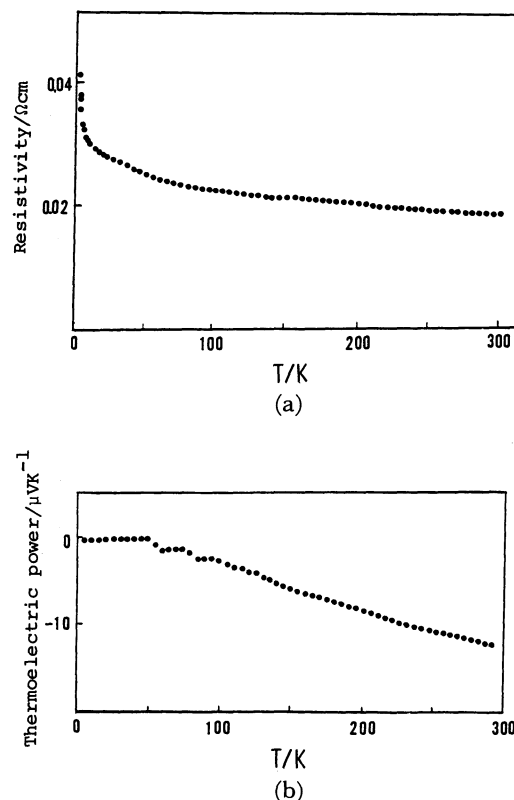


Fig. 2. a) Electrical resistivity of metallic crystalline solid. b) Thermoelectric power ( $\text{S}/\mu\text{VK}^{-1}$ ) of metallic crystalline solid.

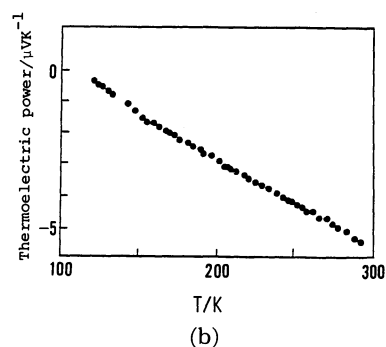
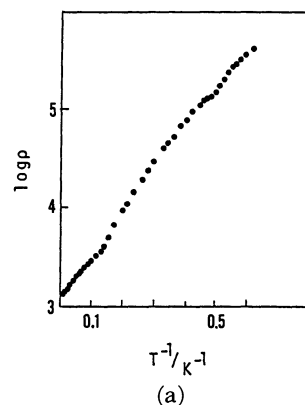


Fig. 3. a) Electrical resistivity of semiconducting solid. b) Thermoelectric power of semiconducting solid.

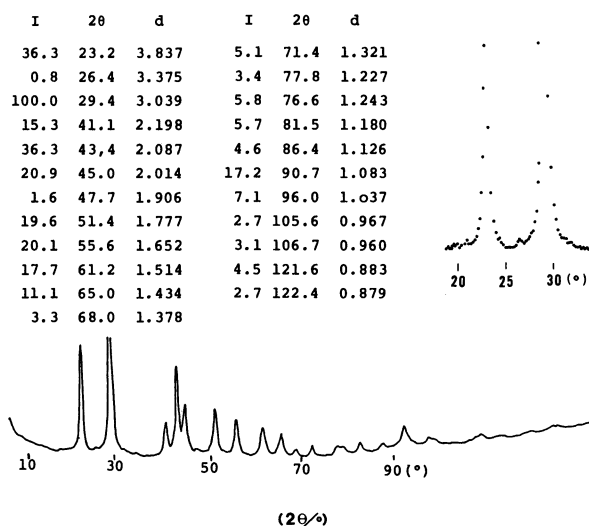


Fig. 4. Lattice spacings ( $d/\text{\AA}^{-1}$ ), intensities (I) and diffraction powder patterns of metallic crystalline solid. The small peak around  $26^\circ$  ( $\text{Cu } K\alpha$ ) seems to be 002 reflection from graphite.

dependence of the thermoelectric power described later suggests that the highly conducting sample is essentially metallic.

Besides the highly conducting samples, there are insulating, low-conducting and semiconducting samples. The conductivity of the insulating sample, which gave amorphous X-ray halos (Fig. 1c) was less than  $10^{-8} \text{ S cm}^{-1}$  and that of the semiconducting sample was about  $5 \text{ S cm}^{-1}$  with activation energy of 0.09 eV (Fig. 3a). The semiconducting solid gave extremely broad Debye rings suggesting the heavily disordered lattices (Fig. 1b). The conductivity of the samples obtained by reheating the insulating sample up to  $250^\circ\text{C}$  is ca.  $10^{-3} \text{ S cm}^{-1}$ , almost identical to the conductivity of poly(carbon diselenide) reported by Okamoto and Wojciekowski.<sup>1)</sup> The low-conducting material was almost amorphous to X-ray diffraction (Fig. 1d). These facts indicate that the solid is metallic in an ordered crystalline state and it becomes less conductive when crystalline imperfection increases. The X-ray powder pattern of the crystalline material was measured on the X-ray diffractometer and more than twenty peaks were obtained. The lattice spacings and the X-ray powder patterns are shown in Fig. 4. The thermoelectric power of the crystalline solid was negative and as small as  $-12 \mu\text{V/K}$  at room temperature. The almost linear temperature dependence suggests the existence of negative free carriers (Fig. 2b).

The IR spectrum of the insulating sample showed the absorption bands at 880, 1260, and  $1380 \text{ cm}^{-1}$ . The strong band at  $880 \text{ cm}^{-1}$  was assigned to the  $\text{C}=\text{Se}$  stretching vibration. The conducting sample was opaque down to at least  $400 \text{ cm}^{-1}$  probably due to the free carrier absorption.

The Fourier transform of EXAFS spectra of the metallic sample was different from that of insulating

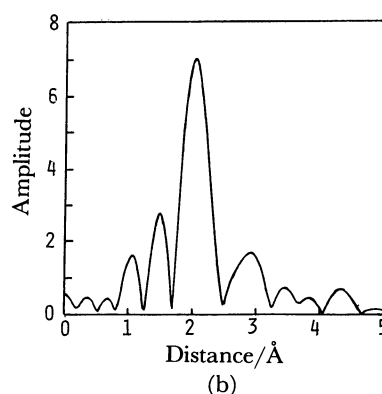
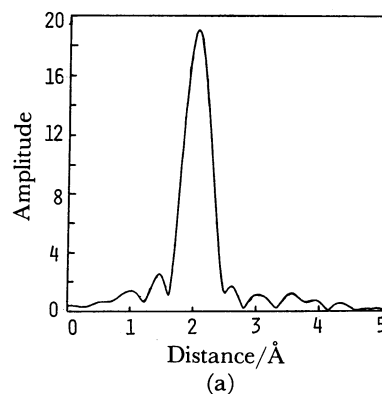


Fig. 5. Fourier transform of the EXAFS oscillation,  $k^3\chi(k)$  for (a) metallic and (b) insulating solids.

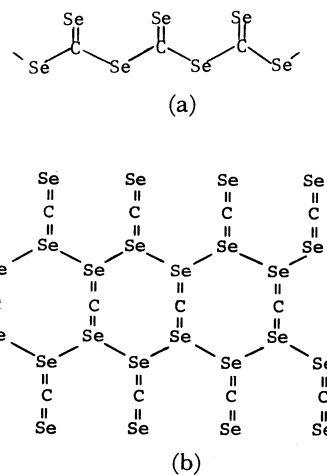


Fig. 6. Structure model of  $(\text{CSe}_2)_x$  polymer. a): Chain structure model<sup>1)</sup> b): Two-dimensional structure model.<sup>6)</sup>

sample but was quite similar to that of hexagonal Se powder (Fig. 5). The prominent peak in the Fourier transform of metallic sample corresponded to Se-Se bond. But no indication of Se-C or  $\text{Se}=\text{C}$  bond was found except in the insulating sample. The bond distances and coordination numbers were obtained by the curve-fitting analyses with empirical parameters. Since hexagonal Se had a helical structure of Se-Se distance of  $2.37 \text{ \AA}$ , the coordination number of Se in

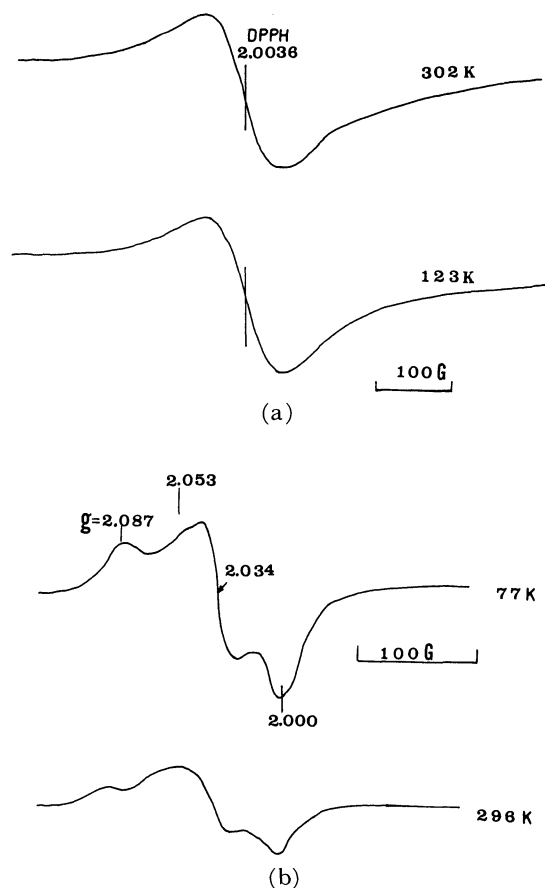


Fig. 7. ESR spectra of a) metallic and b) insulating high pressure reaction products of  $\text{CSe}_2$ .

hexagonal Se was fixed as 2.0. The coordination number of metallic sample was almost 2.0, which indicates that each Se atom has two neighbouring Se atom. Insulating sample had the coordination number of 0.7, but Se-Se distances were almost the same for all the samples. Since the result of EXAFS analyses indicated the existence of  $-\text{Se}-\text{Se}-$  (2.37 Å) infinite chains in the metallic sample, the chain structure model proposed by Okamoto (Fig. 6a) did not conform with the EXAFS experiments. Thus, two-dimensional structure model with  $-\text{Se}-\text{Se}-$  chains was proposed at this stage (Fig. 6b).<sup>6)</sup> However, further characterization revealed that this structure model was not correct one, which will be mentioned later.

X-band ESR measurements of metallic and insulating powder samples of  $\text{CSe}_2$  solid are shown in Fig. 7. The broad ESR signal (the peak-to-peak linewidth is 98 G) and the  $g$  value of 2.0038, which is very close to that of free electron (2.0023). The temperature was varied within 123–243 K at the interval of 20 K. The peak-to-peak linewidth and  $g$ -value, are almost constant within this temperature range. The lineshape was almost Lorentzian in the measured field range of four times as large as the linewidth. These results support the metallic character of the solid and the existence of the conduction electrons. For insulating

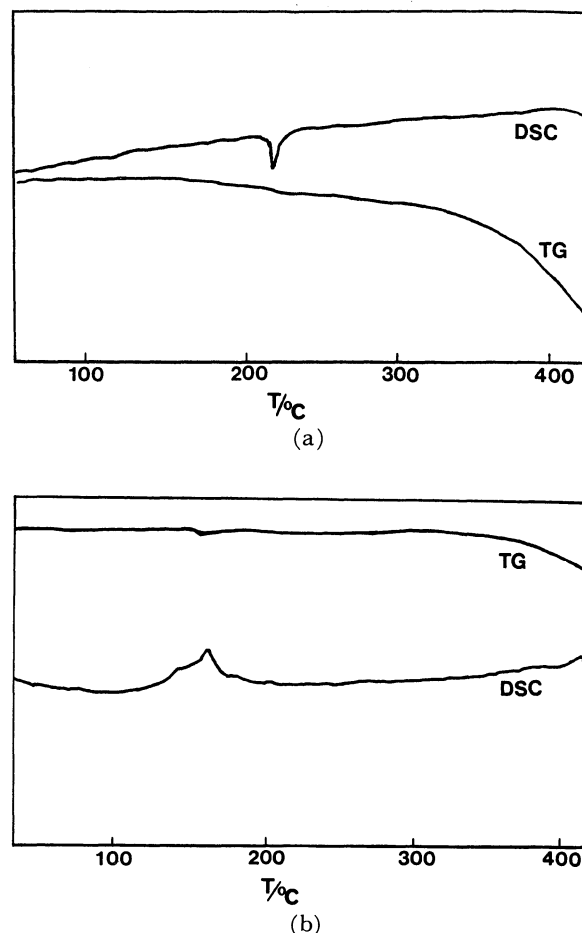


Fig. 8. DSC-TG curves of a) metallic and b) insulating solids.

sample, ESR measurements were performed at room temperature and 77 K. The  $g$ -anisotropic spectra at 77 K indicates that there are more than two radical species. The large  $g$ -shift suggests that these radical species are not C-centered radicals but Se-centered radicals. These ESR measurements indicate that in the metallic sample there exist conduction electrons and in the insulating sample there exist Se-centered radicals produced by broken Se-Se bonds.

Figure 8 shows the DSC-TG curves of the solids. For metallic sample, the endothermic reaction was observed at 220 °C. The thermogravimetric study of the insulating sample showed that three percent of the weight was lost at ca. 160 °C and the remaining was stable up to 300 °C.

In Fig. 9 the magnetic susceptibility of the crystalline sample is shown. From 5 to 296 K the magnetic susceptibility was almost constant and below 5 K the susceptibility increased gradually, which would be an effect of magnetic residuals. The effect of the oxygen molecules included in the sample was observed around 40 K. The magnetic susceptibility performed diamagnetic corrections was  $\chi = -1.75 \times 10^{-6}$  cgsemu  $\text{g}^{-1}$ . The magnetic susceptibility of an electron gas mainly consists of the Pauli paramagnetism and the Landau-

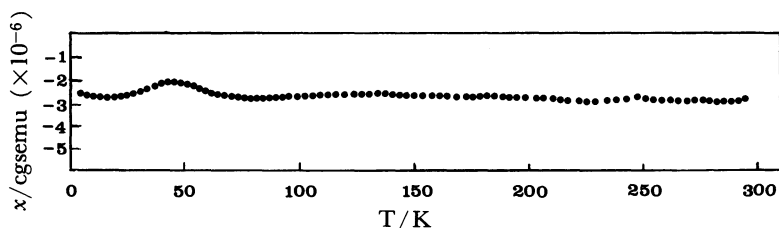
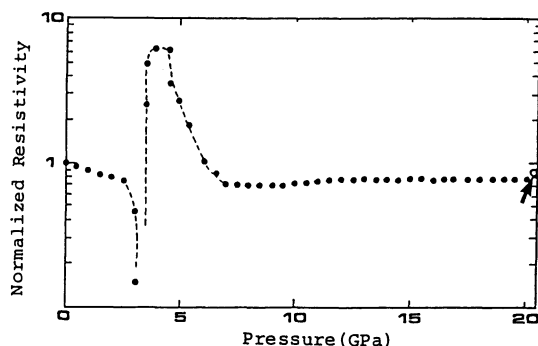


Fig. 9. Magnetic susceptibility of metallic solid.

Fig. 10. The pressure dependence of the normalized room-temperature resistivity ( $\rho(P)/\rho(1\text{Pa})$ ). The open circle indicates the value at 2.1 K obtained by the measurements along the path A shown in Fig. 11.

Peierls diamagnetism. The contribution from Landau-Peierls-Pauli term is represented by<sup>8)</sup>

$$\chi_{\text{LPP}} = \mu_B^2 N / 3\rho\varepsilon_F (3 - \langle f^2 \rangle) F' \varepsilon_F / F k T$$

where  $\mu_B$ : Bohr magneton

$$\langle f^2 \rangle = \text{effective mass correction } (2m_t + m_1) / (m_t^2 m_1)^{1/3}$$

$\chi_{\text{LPP}}$  becomes large negative value, when the second term of above equation is large. The second term is dependent on the anisotropy of the mass. It is well-known that in semimetallic materials such as graphite a large negative magnetic susceptibility is observed due to the large Landau-Peierls term which is derived from the two-dimensional anisotropy. Therefore, it is plausible that metallic crystalline sample has a possibility of having an anisotropic electronic structure.

**Superconductivity at High Pressure.** The high pressure resistivity experiments were performed on the compaction sample by the two probe method using the diamond anvil high pressure cell. The pressure dependence of the room-temperature resistivity is shown in Fig. 10. There was an anomaly around 3 GPa, where a high-conducting state appeared within a small pressure range. Above this anomaly, the solid transformed again into the less conductive state. The resistivity of this high-conducting state was about 10 times smaller than the resistivity at ambient pressure. Above 10 GPa, the pressure dependence of the resistivity became very small. Besides the hysteresis of the 3 GPa transition, the resistivity behavior was almost reversible. The temperature and pressure dependences

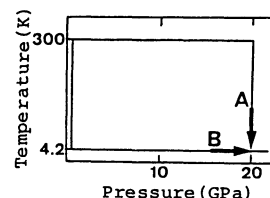
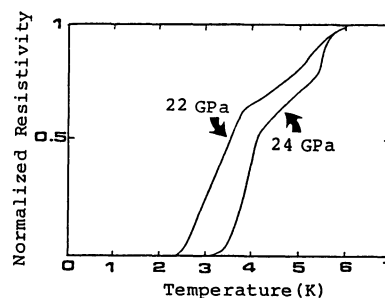


Fig. 11. Two paths (A, B) along which the resistivity measurements were performed.

Fig. 12. Superconducting transition obtained by the measurement along the path B. The ordinate is the normalized resistivity ( $\rho(T)/\rho(6\text{K})$ ).

of the resistivity were measured along two different paths shown in Fig. 11. In the path A, the pressure was increased initially to ca. 20 GPa at room temperature, then the temperature was decreased at constant pressure of ca. 20 GPa. The resistivity at high pressure (20–22 GPa) was almost temperature-independent. Any anomaly was not observed at least down to 2.1 K (the lower temperature limit of the experiment) (Fig. 10).

On the other hand, in the path B, where the temperature was lowered initially and the pressure was increased above 20 GPa with keeping the low temperature, our crystalline sample showed a decrease of the resistivity indicating the onset of the superconducting transition. The result is shown in Fig. 12. Similar dependence of the transition temperature on the measurement process has been also found in black phosphorus.<sup>9)</sup> The superconducting transition temperature of black phosphorus measured along the path B (after temperature was decreased, pressure was increased) was much enhanced than that obtained by the path A (after pressure was increased, temperature was lowered) ( $T_c(25\text{ GPa})=10\text{ K}$  (path B), 6 K (path A)).

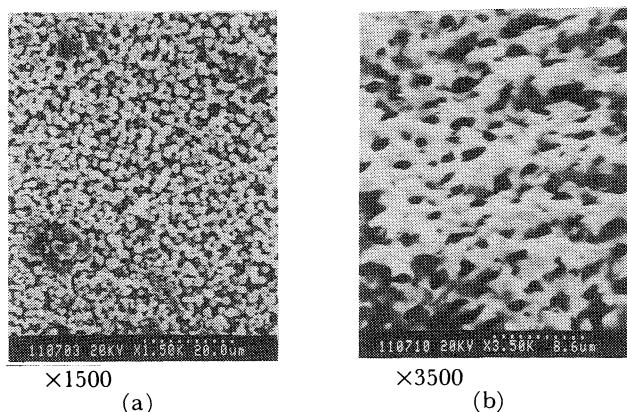


Fig. 13. Photographs of SEM. a) amorphous insulating solid ( $\times 1500$ ) b) metallic crystalline solid ( $\times 3500$ ).

Black phosphorus is considered to be converted into a mixed system consisting of metallic fine threads dispersed in the semiconducting matrix. The appearance of superconductivity in the mixed system by the excitonic mechanism was suggested by Fukuyama.<sup>10)</sup> However, the origin of the enhancement of the transition temperature remains an open questions.

In our crystalline sample, the onset of the superconducting transition was 6 K with the mid-point temperatures of 3.5 K at 22 GPa and 4.1 K at 24 GPa. The temperature range of the transition ( $\Delta T$ ) was fairly large, but the transition became sharp with increasing pressure ( $\Delta T=2.7$  K (22 GPa), 1.9 K (24 GPa)). This superconducting transition of the crystalline sample reminds us of those of various kinds of selenium by ordinary path A. Amorphous Se undergoes a semiconductor to metal transformation at a pressure of 13 GPa and at 7 K superconductivity was observed.<sup>11)</sup> Monoclinic Se has a discontinuity in resistance near 15 GPa, as in amorphous Se. Superconducting transition has onsets at 7 K, but never complete.<sup>11)</sup> Pure hexagonal Se was pressurized to about 16 GPa, no sharp semiconductor to metal transition was observed at any pressure, and at high pressure no superconductivity was found to 1.5 K.<sup>11)</sup>

**Decomposition Reaction of  $\text{CSe}_2$ .** The physical properties and the structure of the black solids obtained by the high pressure reaction of  $\text{CSe}_2$  were examined by several methods as described above. EXAFS indicated the existence of an infinite  $-\text{Se}-\text{Se}-$  chain in the metallic sample, which showed that the  $(\text{CSe}_2)_x$  chain model (Fig. 6a) was not correct at least for the high conducting samples. Thus, we proposed two-dimensional structure model of  $(\text{CSe}_2)_x$ . However, recent examination of the metallic samples have revealed the existence of the crystals of hexagonal Se. Except for the appearance of the small peak around  $26^\circ$  ( $\text{Cu } K\alpha$ ) and large intensities of the peaks around  $90^\circ$ , the X-ray diffraction patterns of the metallic sample (Fig. 4) are almost identical to that of hexagonal Se

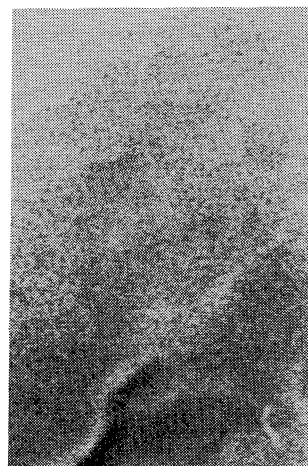


Fig. 14. Photographs of metallic crystalline solid by the electron microscope ( $\times 1500000$  magnification). Crystalline parts with lattice spacings of  $\approx 3 \text{ \AA}$  and some amorphous or cluster regions are observed.

crystal. Since hexagonal Se is not high conductive, the metallic nature of the reaction product seems to be puzzling. However, DSC of the crystalline sample gave another evidence of the existence of hexagonal Se crystals. An endothermic peak was observed around the temperature of the m.p. ( $220^\circ\text{C}$ ) of the hexagonal Se crystal. The photographs of SEM showed that the amorphous insulating solid was composed of the spheres with diameter of about  $13000 \text{ \AA}$ , while the metallic solid appeared to be composed of the uniform black flakes ( $\times 3500$ ) (Fig. 13). However, recent electron microscope ( $\times 1500000$  magnification) and electron diffraction experiments (Fig. 14) have suggested the existence of graphite, which is consistent with the appearance of the small peak around  $26^\circ$  ( $d=3.375 \text{ \AA}^{-1}$ , the strongest peak of graphite crystal) in the X-ray powder diffraction. The electron microscope photographs show that the metallic solid is composed of the crystalline regions and the amorphous or cluster ones. Although the patterns of the electron diffraction and microscope photographs are not simple,<sup>12)</sup> the conducting product could be characterized fairly satisfactorily. There are considerable amount of evidences showing the existence of hexagonal Se. Graphite powder seems to also exist. The value of magnetic susceptibility is plausible for that of graphite. If we assume magnetic susceptibility is derived from almost graphite, it will be  $-24.8 \times 10^{-6} \text{ cgsemu g}^{-1}$ . Thus we may say that the unexpected novel reaction took place. Contrary to the expected polymerization reaction,  $\text{CSe}_2$  is decomposed into the component atoms to produce crystalline hexagonal Se with small crystal size ( $< 500 \text{ \AA}$ ), graphite and some amorphous solids or clusters. Although there exist considerably large amorphous (or cluster) regions, any conductive anomaly was not observed around the pressure where the insulating amorphous Se transform into the metallic (or superconducting) state ( $\approx 15 \text{ GPa}$ ). Therefore, it may be

unlikely that there are large amount of amorphous Se. The high conductivity and the diamagnetism seems to come from the properties of the graphite and the superconductivity from crystalline hexagonal Se. Thus our experiment seems to indicate that superconducting transition of hexagonal Se occurs at the pressure greater than 20 GPa and this may be the first observation of the superconducting transition of hexagonal Se.

However, there remain unsolved interesting features concerning the superconducting transition:

(1) Superconductivity was observed only along the path B. What is the mechanism of the enhancement of  $T_c$ ? Is it plausible that the superconducting transition occurs under 2.1 K (lower limit of the experiments) along the path A and is observed at 2.5–6 K along the path B by the enhancement of the superconducting transition temperature?

(2) Why the transition occurs stepwise (Fig. 12)? The sharpening of the transition with increasing the pressure seems to indicate the increase of the onset temperature of the second step, which shows that there exist two situations of the solid which have different superconducting transition temperatures individually. Since the onset temperature of 6 K resembles that of the transition of Se, what is the origin of the transition with onset temperature of 3.5 K? Further, what is the reason of the partial occurrence of the superconducting transition of 6 K?

In this paper, we presented a novel decomposition reaction of  $\text{CSe}_2$  and the characterization of the conducting solid product. What triggers the decomposition of  $\text{CSe}_2$  and systematic recombination of the component atoms? What is the mechanism of the abnormal superconducting behavior? These problems are open questions.

The authors (A. K. and H. K.) are grateful to Prof.

Okamoto of Polytechnic Institute of New York for helpful discussions about the possibility of the decomposition reaction of  $\text{CSe}_2$ . They are also much obliged to the members of the Application Laboratory of the Hitachi Naka Works for the assistance of the electron microscope and diffraction experiments.

## References

- 1) Y. Okamoto and P. S. Wojciechowski, *J. Chem. Soc., Chem. Commun.*, **1982**, 386.
- 2) R. L. Greene, G. B. Street, and L. J. Suter, *Phys. Rev. Lett.*, **34**, 577 (1975).
- 3) E. Whalley, *Can. J. Chem.*, **38**, 2105 (1960).
- 4) H. Kobayashi, T. Mori, R. Kato, A. Kobayashi, Y. Sasaki, G. Saito, and H. Inokuchi, *Chem. Lett.*, **1983**, 1407.
- 5) H. Kobayashi, A. Kobayashi, and Y. Sasaki, *Mol. Cryst. Liq. Cryst.*, **118**, 427 (1985).
- 6) A. Kobayashi, N. Sasagawa, Y. Sasaki, K. Asakura, T. Yokoyama, H. Ishii, N. Kosugi, H. Kuroda, and H. Kobayashi, *Chem. Lett.*, **1985**, 1.
- 7) W. Pan, and J. P. Fackler, Jr., *Inorg. Synth.*, **21**, 7 (1982).
- 8) W. Sasaki, and J. Kinoshita, *J. Phys. Soc. Jpn.*, **25**, 1622 (1968).
- 9) H. Kawamura, I. Shirotni, and K. Tachikawa, *Solid State Commun.*, **49**, 879 (1984); *ibid.*, **54**, 775 (1985).
- 10) H. Fukuyama, *J. Phys. Soc. Jpn.*, **51**, 1709 (1982).
- 11) A. R. Moodenbaugh, C. T. Wu, and R. Viswanathan, *Solid State Commun.*, **13**, 1413 (1973); J. Wittig, *J. Chem. Phys.*, **58**, 2220 (1973).
- 12) Professor Okamoto suggested the existence of  $(\text{CSe})_x$  polymer, which is very interesting from the view-point of the molecular designing. However, direct evidence of the existence of such a polymer could not be found in our experiments. Unlike the relatively simple X-ray diffraction patterns, the electron diffraction patterns show some extra reflections other than those from hexagonal Se and graphite crystals. Probably oxidation of the surface of the powdered solid will be responsible for the appearance of the complex electron diffraction patterns.